Teletraffic Engineering for Direct Load Control in Smart Grids

Giovanni Neglia, Laura Giarré, Ilenia Tinnirello, Giuseppe Di Bella

Teletraffic Engineering for Direct Load Control in Smart Grids

G. Neglia[a], L. Giarré[b], I. Tinnirello[c], G. Di Bella[c]

[a] *Université de la Côte d'Azur, Inria, Sophia-Antipolis Méditerranée, France - giovanni.neglia@inria.fr*
[b] *Dipartimento di Ingegneria "Enzo Ferrari", Università di Modena e Reggio Emilia, Via Vivarelli 10, - 41125, Modena, Italy - Laura.Giarre@unimore.it*
[c] *Dipartimento di Energia, Ingegneria dell'Informazione, Modelli Matematici, Università di Palermo, Viale delle Scienze - 90128, Palermo, Italy - gsp.dibella@gmail.com, ilenia.tinnirello@unipa.it*

Abstract

The traditional paradigm for power grid operation is to continuously adapt energy production to demand. This paradigm is challenged by the increasing penetration of renewable sources, that are more variable and less predictable. An alternative approach is the *direct load control* of some inherently flexible electric loads to shape the demand. Direct control of deferrable loads presents analogies with flow admission control in telecommunication networks: a request for network resources (bandwidth or energy) can be delayed on the basis of the current network status in order to guarantee some performance metrics. In this paper we go beyond such an analogy, showing that usual teletraffic tools can be effectively used to control energy loads. In particular, we propose a family of control schemes which can be easily tuned to achieve the desired trade-off among resource usage, control overhead and privacy leakage.

Keywords: Smart grid, Direct Load Control, Admission Control, Privacy

1. Introduction

Direct load control (DLC) refers to the possibility of the energy utility (or third-party entities) switching some specific users appliances on and off during peak demand periods and controlling customers electric loads. While at the beginning, DLC was primarily used in critical situations to prevent blackouts by shutting down these loads, more recently, an extensive use of DLC has been proposed as a way to shape energy demand peaks or provide other ancillary services. In [1, 2] for example it has been used to control thermostatic loads, such as air conditioners and heating systems, for a fine-tuning regulation of power demand. Alternative approaches [3, 4] battery-empowered appliances, like electric vehicles, which can act as adaptive loads, but can also re-inject energy in the grid. To respond to different frequency components of the regulation signal [5], multiple load typologies, including deferrable loads such as

pool pumps, have also been considered. Some utilities already employ demand response programs that use deferrable loads to reduce peak demand and manage emergency situations. For example, Florida Power and Light Company has 780'000 customers enrolled in their OnCall Savings Program that implements DLC to households [6]. Users receive in general some economic incentives for their participation in such programs, for example in terms of energy cost reductions. The design of such economic incentives is itself an open research problem (see for example [7] and references therein). The energy management of a smart city can be addressed in several other ways; for example, in [8] a decision process may support the city energy manager and local policy makers in taking energy retrofit decisions, while in [9], a fully distributed peer-to-peer (P2P) architecture is designed to implement distributed demand response schemes in a community of smart buildings.

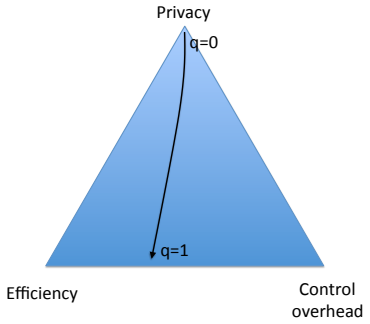

Figure 1: Different trade-offs among efficient resources' usage, control overhead and privacy leakage achievable by tuning the parameter q.

In this paper, we consider a scenario where DLC functionalities are deployed to a large set of small deferrable energy loads, i.e. loads of residential users whose power demand can be postponed but not interrupted, or, in general, modulated, and we propose simple control approaches based on teletraffic engineering. These approaches rely on asymptotic results and are then suited to be applied to large scale systems. Similar to communication networks where data traffic from different sources is multiplexed at routers of different hierarchical levels, indeed, loads on the electrical grid are multiplexed at different aggregation levels (*e.g.*, distribution transformers, primary stations). The required additional intelligence and communication capabilities may be introduced through *smart plugs* [10], without the need to replace older "dumb" appliances. Smart plugs are inserted between the appliance plugs and the power sockets and are already produced with a variety of different purposes: to prevent vampire power drain, monitor energy usage and generally reduce the overall costs of running various electronics. Hereafter, we propose a simple control mechanism that ensures that the instantaneous power demand exceeds a given bound with probability smaller than ϵ, requiring only a stochastic characterization of the power demand for each class of appliances. This mechanism combines two different operational modes. In the first one, appliances need to ask a controller for permission to start, while

the controller limits the number of simultaneously active appliances to $n(t)$. In the second one, an activation probability function—$p(t)$—is periodically broadcast to all the appliances; the appliances can start immediately with probability $p(t)$ or postpone their decision to time $t+T$ with probability $1-p(t)$, without the need to communicate to the controller. The first operation mode requires more communication exchanges between the appliances and the controller and can leak more sensitive information about the users' habits. The second mode works in an open-loop fashion and, then, does not reveal any private information. At the same time, without an exact knowledge of the current number of active appliances, the system will in general require a lower utilization of the resources to satisfy the constraint. In the present paper, we combine the two operation modes by means of a probability q: when an appliance wants to start its operation, it will ask authorization from the controller with probability q, but autonomously deciding to use the function $p(t)$, with probability $1-q$. We achieve the wished trade-off between privacy leakage, resource usage and control overheads through a particular choice of the parameter q. By increasing q we i) reduce privacy by increasingly exposing the energy profile of each user, ii) increase the efficiency, iii) increase control overheads because the controller needs to directly interact with a larger number of appliances. This effect is depicted in Fig. 1, while our analysis (Section 3) and experimental results (Section 5) allow us to quantify these trade-offs.

Rather than presenting a fully developed DLC solution, the main contribution of this paper is to show how teletraffic engineering tools can be advantageously used in the context of future smart power grids. A few papers [11, 12, 13] have already advocated the use of teletraffic tools, but we are the the first to study the application of admission control techniques. For example, network calculus has been proposed to size transformers [12] and energy batteries [11]. Queuing theory is also used in our paper [13] for sizing the population of customers subscribing a DLC program under a given maximum activation delay for the appliances.

Our system is described in Section 2 where we analyze our mechanism, and the control policy, determined by the two functions $p(t)$ and $n(t)$. In Section 3, we show how techniques developed in literature for flow admission control in data networks can be here used to determine a stationary control policy (*i.e.*, $p(t)=p$ and $n(t)=n$ when the appliances' activation rate is assumed to be time-invariant). In Section 4, we derive the time-variant control policies for the more realistic case when the appliance activation rate i) is time-varying and ii) needs to be estimated.

This paper extends our conference version [14] in a number of directions: i) it includes the proof of Proposition 1, ii) it studies a different constraint on the power demand profile defined through an energy bucket, iii) it provides more insights on resources' utilization with new numerical results as well as additional discussion in Appendix A, iv) it studies the communication overhead of the proposed solution.

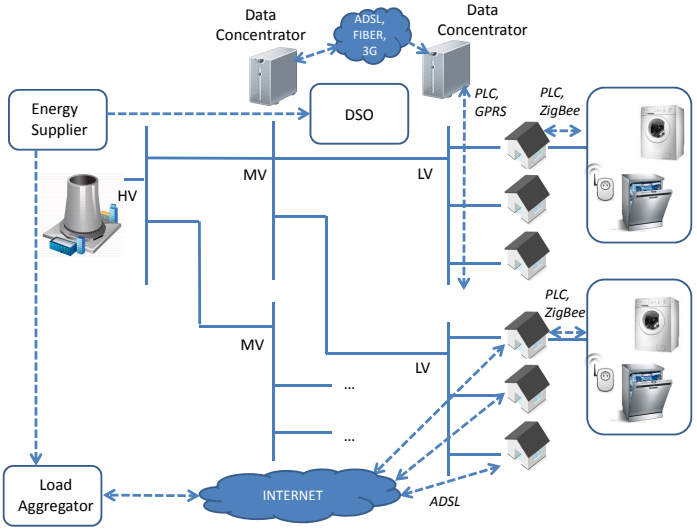

Figure 2: Reference scenario: communication infrastructure and control system for DLC managed by a DSO and/or a load aggregator.

2. System Description

We consider the problem of peak shaving: an energy supplier wants to reduce its customer power consumption when energy costs are higher. To achieve these goals, the energy suppliers can interact with the distribution system operators (DSO), and/or with novel intermediate figures called load aggregators [15] by means of a communication infrastructure transporting the control messages. Both possibilities are illustrated in Fig. 2 where dashed lines indicate control message flows. The solution based on the DSO can take advantage of broadcast functionalities deployed at the data concentrators. In fact, broadcasting of low-rate control signals can be very efficiently performed by power line communications (PLCs) in the low-voltage (LV) distribution grid [16]. The aggregator can exploit standard Internet connectivity to interact with appliances at customer premises. The two approaches can coexist, and our solution can operate in both scenarios. This is the reason why we will generically refer to the entity (DSO or load aggregator) which drives the appliances as the load controller.

An energy supplier can interact with different load controllers. It specifies a high-level requirement for each controller in terms of a maximum probability to exceed a given power demand in the controlled area. Each load aggregator is responsible to meet its request by driving the activation of deferrable loads, such as dish-washers and laundry machines, in the controlled area. Because each load controller independently acts from the others, in this paper we can focus on a single load controller. On the basis of the demand forecast, the load controller maps the requirements into a control signal that is transmitted

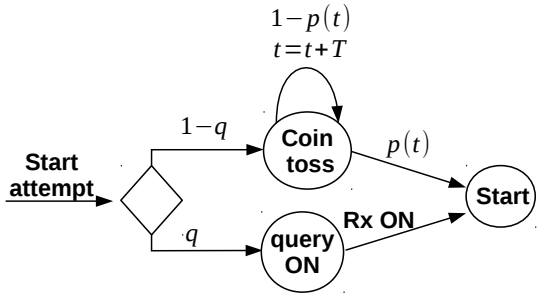

Figure 3: Household control model in terms of activation probability $p(t)$ and ratio of forwarded queries q.

to all the controlled households to decide if deferring or not load activation requests. Each household is equipped with a gateway able to receive the control signal and to communicate with the domestic appliances by means of local area technologies (such as ZigBee or PLC). Smart appliances can be able to directly interact with the gateway, while dumb appliances can be controlled by means of smart plugs [10].

In our control system, the signal broadcast by the load controller represents the probability $p(t)$ to accept or postpone a load activation request during the intervals of the day. At each household, the gateway can autonomously decide about a novel activation request on the basis of this function: the request is accepted with probability $p(t)$ and deferred of a fixed time interval T with probability $1-p(t)$. This operation applies to a fraction $1-q$ of all the requests. The others are directly forwarded to the load controller and the gateway waits for an acknowledgment signal (ACK) from the load controller before accepting the request. The controller maintains a cap $n(t)$ on the number of appliances active at a given time instant (among those it is aware of, i.e. those whose activation request has been sent to the controller). The ACK can then be delayed until some operating appliance does not finish. This mechanism allows the load controller to estimate the time-varying power demand, but also to have a tighter control on the aggregate power demand and then to achieve a more effective resource utilization in the controlled area.

Figure 3 describes the actuator model at the household: different control modes can be programmed by the load controller by tuning q and $p(t)$. For example, when q is set to 1, all the activation requests are forwarded to the load controller by means of unicast transmissions. This implies a better control on the aggregated power demand, because the number of active appliances is known and the only source of randomness is due to the appliance consumptions. On the contrary, when q is very small, most of communications are unidirectional (from the load controller to the households), while decisions can be locally taken with minimal delays. However, the aggregate power consumption is affected by two sources of randomness (the one related to the number of appliance active, and the other one related to the appliance consumption) which require a lower

admission rate for not exceeding the power constraint.

3. Control in a Stationary Setting

We aim at designing a direct load control system capable to enforce a given threshold on the overall power absorbed from a set of appliances with known statistical properties. We assume that the appliance power consumptions are i.i.d. non-negative random variables $\{X_i\}$ with density function equal to $f_X(x)$. The only requirement about the distribution of X is that its cumulant generating function $M_X(s) := \ln \mathbb{E}[e^{sX}]$ is finite in a neighborhood of 0. We use $\mathbb{E}$ to denote expectation.

Let $A(t)$ be the set of active appliances at time t, with $|A(t)| = m(t)$. The total absorbed power is $P(t) = \sum_{i \in A(t)} X_i$. First, we consider that the energy supplier wants to guarantee that $P(t)$ does not surpass the threshold $\bar{P}$ with probability larger than ϵ, i.e.:

$$\Pr\left(\sum_{i \in A(t)} X_i > \bar{P}\right) \leq \epsilon. \tag{1}$$

Then, in Section 3.4, we show how similar results can be derived for a different type of constraints on $P(t)$. We observe that if the energy provider can interact with L load controllers in a given area, then it will need to define a specific pair of requirements $(\bar{P}_l, \epsilon_l)$ for each load controller $l \in \{1, 2, \ldots L\}$, so that $\Pr\left(\sum_{i \in A_l(t)} X_{i,l} > \bar{P}_l\right) \leq \epsilon_l$. A simple way to guarantee that (1) is satisfied is to choose the bounds $(\bar{P}_l, \epsilon_l)$ so that $\sum_{l=1}^{L} \bar{P}_l = \bar{P}$ and $\sum_{l=1}^{L} \epsilon_l = \epsilon$. This choice implicitly considers a worst-case situation where the bounds are violated at the same time at all the load controllers. This configuration rule can be acceptable if the number of load controllers in the area is small, as it will probably be the case in the near future. For a large set of load controllers, the choice can be too conservative, but it is then possible to use more sophisticated rules from the teletraffic theory as acceptance regions for multi-type flows (see for example [17, Sec. 6.2].

3.1. Classic large deviation results in the $q = 1$ case

If $q = 1$, i.e. if all the queries are forwarded to the controller, we need to determine the maximum value n, such that

$$\Pr\left(\sum_{i=1}^{n} X_i > \bar{P}\right) \leq \epsilon. \tag{2}$$

The same problem has been considered in telecommunication networks to configure Call Admission Control (CAC) mechanism. The purpose there is to determine the maximum number n of homogeneous data flows, each with instantaneous rate X_i in order to guarantee that the traffic on a link exceeds the value $\bar{P}$

(e.g. the link capacity) with probability at most ϵ. Even if different approaches have been proposed to set the value of n, here, we introduce a simple one based on large deviation results (see e.g. [17, Ch. 6]), but more sophisticated techniques can also be applied [18]. Our main goal in this paper is to show how teletraffic tools can in general be reused in this different context, rather than specifically develop the solution in all its details.

From the Chernoff bound and basic properties of the cumulant generating function, it follows that:

$$\ln \Pr(X_1 + ... + X_n > nc) \leq n \inf_{s \geq 0} [M_X(s) - sc] \tag{3}$$

Moreover, Cramer's theorem proves that this bound is asymptotically tight:

$$\lim_{n \to \infty} \frac{1}{n} \ln \Pr(X_1 + ... + X_n > nc) = \inf_{s \geq 0} [M_X(s) - sc] \tag{4}$$

Practically speaking, when n is large, Cramer's theorem is used to approximate the probability that the sum of n independent random variables exceeds a bound ($\bar{P}$ in our case) as follows:

$$\ln \Pr(X_1 + ... + X_n > \bar{P}) \approx \left(\inf_{s \geq 0} [nM_X(s) - s\bar{P}] \right),$$

and then n can be determined as the largest integer such that

$$\left(\inf_{s \geq 0} [nM_X(s) - s\bar{P}] \right) \leq \ln \epsilon.$$

The set of values $\{0, 1, \ldots, n\}$ is called the *acceptance region* for the admission controller.

The approach can be easily generalized to a finite number of appliance classes and the concept of *effective bandwidth* can be defined for each class in order to easily derive a subset of the acceptance region [17, Ch. 6].

3.2. Extension to $q < 1$

As we are going to discuss in what follows, the results above can be extended to the scenario where a subset of the appliances does not query the controller, but autonomously starts its operation. For the moment, we assume that appliances would like to activate according to a Poisson process with constant rate λ and we ignore retrials. Then, there is a request process with rate $q\lambda$ to the query-response system, and a spontaneous activation process of appliances with rate $\lambda_c = p(1-q)\lambda$, both of which are Poisson processes. The probability p is considered to be constant for the moment. In the following Section 4 we take into account the exogenous time-variant activation process as well as the retrial mechanism. For the sake of simplicity, let us assume that all the appliances have the same activation time equal to D, but the analysis can be easily carried on also when D is a random variable.

Let N denote the random number of appliances autonomously starting. Under the assumptions indicated above, N is distributed as a Poisson random variable with parameter $\Lambda_c := \mathbb{E}[N] = \lambda_c D$. The condition in (2), then becomes

$$\Pr\left(\sum_{i=1}^{n} X_i + \sum_{j=n+1}^{n+N} X_j > \bar{P}\right) \leq \epsilon. \tag{5}$$

Large deviation results hold for large systems, for example when both the number of random variables (n) and the threshold to be exceeded (nc) diverge as in (4). In (5) both the first and the second addend should scale in the same way, otherwise one of them would become negligible in comparison to the other. We assume then that the mean Λ_c of the number of appliances autonomously starting scales linearly with n: $\Lambda_c = n\Lambda_c^0 = n(1-q)pD\lambda_c^0$, where we also took into account λ_c's dependence on p and $1-q$. It is then possible to prove the following result:

Proposition 1. *Let $(X_i)_{i\in\mathbb{N}}$ be a sequence of independent and identically distributed random variables with cumulant generating function $M_X(s)$, and N be a Poisson random variable with mean $n\Lambda_c^0$. We assume that $M_X(s)$ is finite in an interval around $s = 0$ and $\Pr(X > c) > 0$. It holds:*

$$\lim_{n\to\infty} \frac{1}{n} \ln \Pr\left(\sum_{i=1}^{n} X_i + \sum_{j=n+1}^{n+N} X_j > nc\right) = \inf_{s\geq 0} \left[M_X(s) + \Lambda_c^0 \left(e^{M_X(s)} - 1\right) - sc\right].$$

Proof. Let us define $\{Y_{i,k}, i = 1, \dots n, k \in \mathbb{N}\}$ to be a set of independent random variables with the same distribution as X and $\{N_i, i = 1, \dots n\}$ to be a set of independent Poisson random variables with mean Λ_c^0. The sum of the variables N_i has the same distribution of N and then:

$$\sum_{i=1}^{n} \sum_{k=1}^{N_i} Y_{i,k} \stackrel{d}{=} \sum_{j=n+1}^{n+N} X_j.$$

Let $Z_i \triangleq X_i + \sum_{k=1}^{N_i} Y_{i,k}$, for $i = 1, \dots n$. It follows that

$$\sum_{i=1}^{n} Z_i \stackrel{d}{=} \sum_{i=1}^{n} X_i + \sum_{j=n+1}^{n+N} X_j.$$

All the variables Z_i are independent and identically distributed with cumulant generating function $M_Z(s) = M_X(s) + \Lambda_c^0 \left(e^{M_X(s)} - 1\right)$. The thesis follows by directly applying Cramer's theorem to $\sum_{i=1}^{n} Z_i$. □

In a finite-size system, this result is used to approximate the probability that the total power consumption exceeds the bound $\bar{P}$ as follows:

$$\ln \Pr\left(\sum_{i=1}^{n} X_i + \sum_{j=n+1}^{n+N} X_j > \bar{P}\right) \approx \inf_{s\geq 0}\left[nM_X(s) - \lambda_c D\left(e^{M_X(s)} - 1\right) - s\bar{P}\right]. \quad (6)$$

and then the acceptance region is made by all the pairs of values (p, n) such that:

$$\inf_{s\geq 0}\left[nM_X(s) + \lambda_c D\left(e^{M_X(s)} - 1\right) - s\bar{P}\right] \leq \ln \epsilon, \quad (7)$$

where $\lambda_c = p(1-q)\lambda$. In the next subsection, we characterize such region for a simple case.

3.3. An illustrative toy example

In order to better explain the admission control rule derived above, we consider a toy example where there is a single class of appliances, which would like to activate according to a Poisson process with rate $\lambda = 12$ appliances per minute. The appliance stays in the high consumption state on average 10 minutes and consumes 1.5kW, it stays in the low consumption state on average 20 minutes and consumes 500W. Literature indeed suggests that Markov processes can accurately model appliance consumption [19].

For this appliance, the cumulant generating function can be easily calculated as $M_X(s) = \ln\left(1/3e^{s1.5} + 2/3e^{s0.5}\right)$. Then inequality (7) can be used to determine the acceptable pairs (p, n) with $\lambda_c = p(1-q)\lambda$:

$$\inf_{s\geq 0}\left[nM_X(s) + p(1-q)\lambda D\left(e^{M_X(s)} - 1\right) - s\bar{P}\right] \leq \ln \epsilon. \quad (8)$$

Fig. 4 shows the frontiers of 10 different acceptance regions calculated for $\lambda = 12$, $D = 90$ minutes, $q = 0.1, 0.2, \ldots, 1$, $\epsilon = 0.1$ and $\bar{P} = 0.75\lambda D\ \mathbb{E}[X]$ (the 80% of the average absorbed power in absence of the control). Each curve[1] is made by the pairs (p, n) for which the constraint in (7) is satisfied with an equality. The acceptance region is then made by all the points that are below this curve. This is analytically evident because the left term in (8) is increasing in n and p, but it is also intuitively clear because of the physics of the system: for a given acceptable pair (p, n), if we limit more p or n ($p' < p$ or $n' < n$), then less appliances will be admitted in the system and the constraint will be even more satisfied (both (p', n) and (p, n') are acceptable). We observe the expected trade-off between n and p: on the frontier as n increases, p needs to decrease. The more appliances we decide to admit through the query-response system, the more we have to limit through p the expected number of appliances which will autonomously activate.

[1] Obviously n can only assume integer values, but here we are considering a continuous relaxation. In practice, the values can then be lower-rounded.

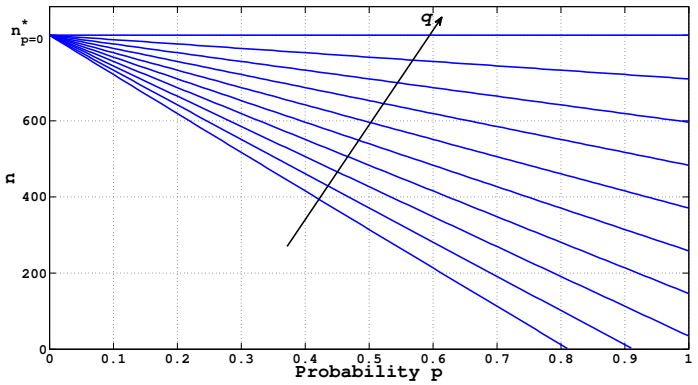

Figure 4: Acceptance regions of the pairs (p, n) for different values of the querying probability q.

Another interesting remark about the frontiers in Fig. 4 is that they look approximately linear. This can simplify the determination of the acceptance region and leads to important conclusions about the efficiency of resource usage. For this reason, we deeper investigate such behavior. The term $e^{M_X(s)}$ grows very fast for $s \geq 0$ and because of this the point of minimum for the left-hand side of (8) is close to 0, specially for larger $p(1-q)$. It is then possible to consider a first order Taylor approximation $(e^{M_X(s)} - 1) \approx M_X(s)$ and the frontier can be approximated as follows:

$$\inf_{s \geq 0} \left[(n + (1-q)pD\lambda)\, M_X(s) - s\bar{P} \right] = \ln \epsilon,$$

For a given value of q, the frontier is made by pairs (p, n) such that:

$$n + (1-q)pD\lambda = \text{const.} \tag{9}$$

To univocally identify the linear dependance, observe that for $p = 0$ the maximum value for n (let us denote it as $n^*_{p=0}$) does not depend on q, i.e. all the frontiers pass by the point $(0, n^*_{p=0})$ and they are described by the following linear equation parametrized in q:

$$n + (1-q)pD\lambda = n^*_{p=0}. \tag{10}$$

If there are n appliances activated through the query-response mechanism, the expected number of appliances in the system is $n + (1-q)pD\lambda$ and then the expected power consumption is $\mathbb{E}[P] = (n + (1-q)pD\lambda)\mathbb{E}[X]$. This means that for a given q value all the points in the frontier described by (10) have the same aggregate consumption $\mathbb{E}[P] = n^*_{p=0}\mathbb{E}[X]$ while satisfying the constraint. Moreover, for any value of q we can achieve the same power consumption by selecting (n, p) on the corresponding frontier. Although (10) stems from a linear approximation, it suggests that the efficiency (in terms of aggregate power consumption) of our control mechanism is not very sensitive neither to the pair

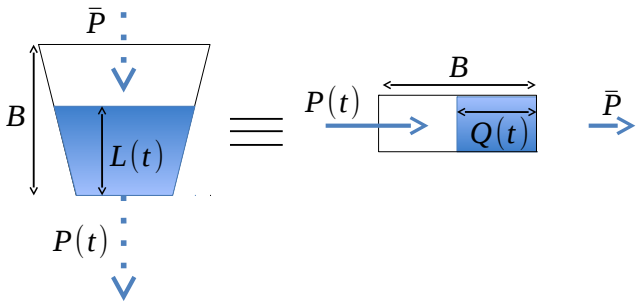

Figure 5: Analogy between the energy bucket on the left and a work-conserving queuing system on the right.

(n, p) (as long as it is a point of the frontier), nor to the parameter q. This is confirmed by our numerical analysis: for example we observed less than 5% reduction of the maximum expected consumption changing q from $q = 1$ to $q = 0$ despite the fact that for $q = 0$ the control needs to deal also with the variability of the number of appliances admitted. However, in practice, direct queries are also needed to accurately estimate the appliance activation rate as discussed in Section 4. Appendix A further discusses the relation between n, p, q and average utilization.

3.4. Long and short power violations

Before describing how the above control policy can actually be used in a case when the activation pattern is time-varying and unknown, we want to briefly show that teletraffic tools can also be used to deal with different constraints. In particular, the constraint $\Pr(P(t) > \bar{P}) \leq \epsilon$ ignores the time duration during which the constraint $\bar{P}$ is violated. It may be significant for the energy utility to target the following different type of constraint.

Let us define an *energy bucket* as follows: the bucket can store an energy capacity equal to B, it is filled with constant rate $\bar{P}$ and emptied with the variable rate $P(t)$. Let $L(t)$ denote the energy stored in the bucket at time t. Fig. 5 describes on the left side the energy-buffer. While inspired by the token-bucket used to shape data traffic, this energy-bucket is only used to express a constraint. If one requires that $L(t) > 0, \forall t$ then $P(t)$ can occasionally exceed the constraint $\bar{P}$ by δP, but only for the time interval $[t, t + L(t)/\delta P]$. The ratio behind such bound is that smaller violations would be tolerated for a longer time. Given the incertitude on the power demand, the control policy cannot guarantee the deterministic bound described above, but rather its probabilistic version:

$$\Pr(L(t) = 0) < \epsilon, \forall t. \tag{11}$$

The possibility to use teletraffic tools (and in particular large deviation results) also to deal with the constraint in (11) derives from the following equivalence: the energy-bucket on the left of Fig. 5 is equivalent to the queue in the same figure on the right, where the input and the output process have been

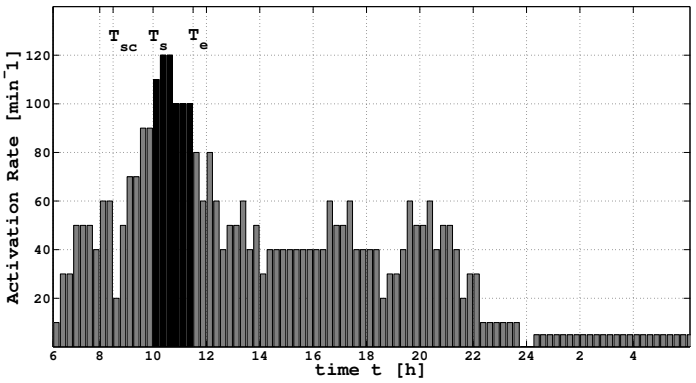

Figure 6: Aggregate activation rate for 30000 washing machines.

reversed, i.e. a traffic with rate $P(t)$ is offered to a queue with service rate $\bar{P}$. Specifically, if $L(0) = B$ and $Q(0) = 0$, then $L(t) = Q(t)$ for every $t \geq 0$. This result is quite evident, but we have not found it in the literature, so we prove it in Appendix B.

The important consequence for our purposes is that controlling the activation of electric appliances so that the aggregate consumption rate satisfies constraint (11) is equivalent to admit data flows to a queue so that the probability to lose packets because of buffer overflow is smaller than ϵ. This problem is also well studied in teletraffic literature and corresponding results can be used also for smart grids.

This example has further shown the potential relevance of applying teletraffic tools to load control in smart grids.

4. Control in a Time-Variant Setting

In this section, we address how our analysis above can be practically used when the appliance activation process is not stationary, its rate is unknown, and probabilistically controlled appliances retry to activate some time later.

Indeed, the usage of electric appliances considerably varies over a day. For example Fig. 6 shows the activation rate of washing machines over 15 minutes intervals, as derived from data in [20]. We need then to take into account the effect of a time-variant activation rate $\lambda(t)$ that is generally unknown even if historical data may be available. We assume that this spontaneous activation process can be modeled as a non-homogeneous Poisson process with rate $\lambda(t)$. Poisson distribution is a standard assumption for an aggregate process arising from many independent decisions. In order to analytically justify this result, it is possible to reason as follow. Let $I_i(t)$ be a random variable indicating if the electric load i is active at time t, ignoring the control action. Clearly the number of loads active at time t is $N(t) = \sum_i I_i(t)$. It is reasonable to assume that the r.v. $I_i(t)$ are independent (each user decides independently to turn on its appliance). Consider then a class of electric loads for which the activation

pattern is similar, the corresponding r.v.s $I_i(t)$ would roughly have the same distribution, hence $N(t)$ can be very well approximated by a Binomial random variable. Finally, given that the set of appliances is large and the probability that a given appliance is active at a given time t is relatively small (e.g. a washing machine is activated a few times per week), we are in the usual scenario where a Binomial r.v. can be approximated by a Poisson r.v. with the same expected value. We remark that the same reasoning has been traditionally used in telephone network dimensioning.

In order to keep track of the dynamics of the activation process, the control policy needs to be time-varying too, i.e. in general we will have $n(t)$ and $p(t)$. We decided to consider $n(t) = \text{const} = n$ and then to compensate for process changes by dynamically tuning $p(t)$. Other choices about how to jointly adapt the two control actions would have been possible and would have lead to different performance in terms of resources' usage, communication requirements (e.g. if p is constant, it does not need to be periodically transmitted) and fairness between the two groups of appliances—those probabilistically controlled and those controlled through query-response—(e.g. in terms of delay before the activation). The control is time-slotted with time intervals of length T_c. We consider that the control starts at time $t = 0$, and we denote by p_k the value of the control action during the k-th time slot, i.e. $p(t) = p_k$ for $t \in [(k-1)T_c, kT_c)$. For the sake of simplicity we will also assume that the retrial delay T is equal to T_c and the activation time (D) of the appliance is a multiple of T_c (i.e. $D = dT_c$), even if the three parameters are in general independent.

Figure 7 shows the system model we are going to describe below. We follow the conventional control theory terminology, where a plant is the combination of the process under control and the control actuator.

The plant is shown in the bottom part of Fig. 7. The input is the spontaneous activation process, i.e. the series of activation instants in absence of any form of control, that, as said above, we assume it can be correctly modeled by a (non-homogeneous) Poisson process with rate $\lambda(t)$. The control system assumes $\lambda(t)$ to be constant during a control slot, while this is not necessarily the case. In Section 5 we address the effect of such an approximation. We denote by λ_k the spontaneous activation rate during the k-th time slot (time dependence is omitted in the figure). The initial requests are randomly split in two independent Poisson processes with rate, respectively, $q\lambda_k$ and $(1-q)\lambda_k$. The rate of appliances that will consider to autonomously activate in slot k is $\lambda_{eq,k}$. It holds:

$$\lambda_{eq,k} = (1-q)\lambda_k + \lambda_{eq,k-1}(1-p_{k-1}), \tag{12}$$

where the first addend is due to all the appliances that are considering to activate themselves for the first time during the k-th time slot, and the second one is due to those that have already considered this decision in the $(k-1)$-th slot and have postponed it to the current one. The actual activation rate of probabilistically

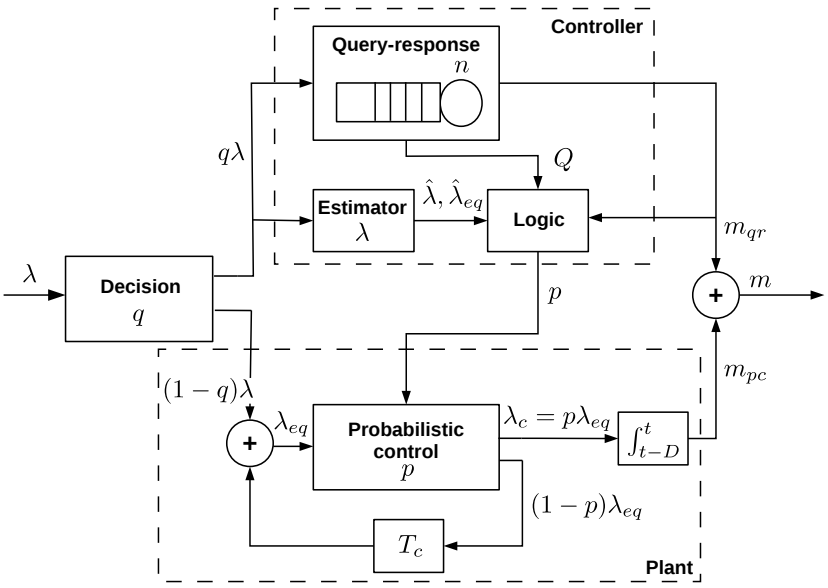

Figure 7: System block diagram.

controlled appliances[2] is $\lambda_{c,k} = p_k \lambda_{eq,k}$. Finally, the actual number of active appliances $m_{pc,k}$ admitted through the probabilistic control and active at time kT_c is equal to those that started during the interval $[kT_c - D, kT_c]$. This is a Poisson random variable with expected value $\mathbb{E}[m_{pc,k}] = \sum_{h=k-d+1}^{k} \lambda_{c,h}$.

The upper part of Fig. 7 describes the controller. It directly receives the activation queries with rate $q\lambda_k$ and it guarantees that the number of appliances active at a given time does not exceed n. Let $m_{qr,k}$ denote the number of appliances controlled through the query-response mechanism and active at time kT_c.

Estimators. The state of the plant (e.g. how many appliances are taking the decision to autonomously activate) is a priori unknown. The controller needs then to estimate the rates λ and λ_{eq}. An estimate for quantity x is denoted as $\hat{x}$. In particular two different sets of estimates will be useful: $\hat{\lambda}^p_k$ and $\hat{\lambda}^p_{eq,k}$ will estimate the sequences until the current slot k, while $\hat{\lambda}^f_{k+1}$ and $\hat{\lambda}^f_{eq,k+1}$ will be used as a prediction for the slot $k+1$ in order to determine p_{k+1}. In this paper we consider simple estimators for these quantities, but we show that they adequately work in Section 5. Given $N_{r,k}$ the number of queries received during the k-th slot, the Maximum Likelihood Estimator for λ_k is simply $\hat{\lambda}^p_k = N_{r,k}/(qT_c)$. Clearly, this estimate could be improved if some *a priori* knowledge is available (e.g. from historical data). The prediction for slot $k+1$ is $\hat{\lambda}^f_{k+1} = \hat{\lambda}^p_k$.

[2] It is possible to show that the point process of such activations is also a Poisson process.

The estimates $\hat{\lambda}^p_{eq,k}$ and $\hat{\lambda}^f_{eq,k+1}$ are obtained as a function, respectively, of $(\hat{\lambda}^p_k, \hat{\lambda}^p_{eq,k-1})$ and of $(\hat{\lambda}^f_{k+1}, \hat{\lambda}^p_{eq,k})$ using (12).

Control logic. The controller determines p_{k+1} on the basis of the acceptance region derived in Section 3. For simplicity we consider a linearized frontier:

$$n + \Lambda_{k+1} = n^{(q)}_{\min} + \lambda_{\max}(1-q)p^{(q)}_{\max}, \tag{13}$$

where Λ_{k+1} is the expected number of active probabilistically controlled appliances at the end of the $(k+1)$-th slot, $\lambda_{\max}$ is the maximum arrival rate in the slot, $n^{(q)}_{\min}$ is the minimum value of n on the frontier (it is 0 if the frontier intersects the segment $[0,1]$), $p^{(q)}_{\max} \triangleq \max\{p | n^{(q)(p)} \geq n^{(q)}_{\min}\}$, i.e. the largest probability value in the frontier. In the experiments below, the parameter n is roughly set to half of the constant on the right hand side. In the stationary case without retrials, it was simply $\Lambda_{k+1} = \lambda_c D = \lambda(1-q)pD$. Here, we can express Λ_{k+1} as the sum of two terms, one (denoted as $\Lambda_{hist,k+1}$) due to all the probabilistically controlled appliances already in the system at the begin of slot $k+1$, the other due to the estimated number of appliances which will activate during slot $k+1$. We can estimate $\Lambda_{hist,k+1}$ as follows $\hat{\Lambda}_{hist,k+1} = \sum_{h=0}^{d-2} p_{k-h}\hat{\lambda}^p_{eq,k-h}T_c$, and then

$$\hat{\Lambda}_{k+1} = \hat{\Lambda}_{hist,k+1} + \hat{\lambda}^f_{eq,k+1}T_c p_{k+1}. \tag{14}$$

Finally p_{k+1} can be iteratively derived from (13) and (14) This may lead to a too conservative strategy, because the number $m_{qr,k+1}$ of active appliances in the query-response queue can be significantly smaller than n, specially at the begin of the control period (the queue fills, initially, with rate λq) and then the configuration above would lead to a severe under use. A solution is to predict the number of active appliances in the query-response queue during the residual control period (i.e. $\hat{m}_{qr,h}$ for $h > k$). Then, p_{k+1} can be calculated replacing n in (13) with the most pessimistic forecast until the end of the control period, i.e. with $\max\{\hat{m}_{qr,h}, h > k\}$. This is the approach we adopted.

5. Numerical Results

In this section we show the performance of the control system described in Section 4 in a realistic setting. In particular we consider a scenario where 30000 washing machines participate to the DLC program. The instantaneous power consumption of a washing machine is assumed to follow the simple model in Section 3.3 and the activation time is $D = 90$ minutes. The spontaneous activation rate $\lambda(t)$ is the one in Fig. 6, derived from experimental data in [20]. The largest expected power demand $P_{\max}$ is at around time 11.00am. We assume the energy supplier sets the constraint as $\Pr(P > \bar{P} = 0.8P_{\max}) < 0.1$ in the interval $[T_s, T_e] = [10.00\text{am}, 11.30\text{am}]$. In order to be sure to satisfy the constraint at $t = 10.00$am, the control needs to start at $T_{sc} = 8.30$am.

Figure 8 plots the evolution of the power demand with and without control for $q = 0.5$ and $T_c = 15$ minutes together with the probability signal $p(t)$. We observe that the controller does not actually intervene ($p(t) = 1$) until

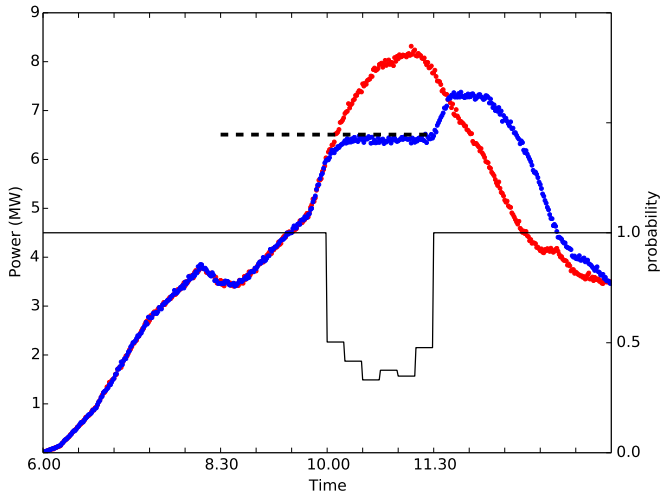

Figure 8: Instantaneous absorbed power (with and without the applied control), and the computed activation probability $p(t)$.

$t = 10.00$am and that it actually manages to maintain the absorbed power below $\bar{P}$ for the whole duration of the control interval. Observe also how power consumption significantly increases after T_e. This is due to the fact that a severe constraint has been imposed for a long time interval. The increase in power demand can be made smooth by gradually increasing $\bar{P}$ after T_e as it is shown in Fig. 9.

The following figures 10 and 11 show the utilization—evaluated as ratio between the average power demand and $\bar{P}$—and the probability to exceed the bound at time $t = 10.26$am estimated over 1000 simulations for different values of $q \in [0, 1]$ and for $T_c = 1, 5, 15, 30$ minutes. The time instant of observation falls in the interval where there is the largest activation rate after a period when the rate has been almost constantly increasing. It is then a particularly critical instant for the control system. All confidence intervals in the figures have 95% confidence level.

The upper plots of figures 10 and 11 correspond to the ideal case when the controller has perfect estimation of the average request rate in the next timeslot, i.e. $\hat{\lambda}^f_{k+1} = \lambda_{k+1}$. We observe that utilization increases as q increases, but no more than 3%. The probability to exceed the bound roughly reflects the same trends, with higher probabilities corresponding to higher utilization. In any case the probability values are well below $\epsilon = 0.1$. The curves almost overlap for all the values of T_c but $T_c = 30$ minutes. This is due to the fact that the actual activation request rate is constant over 15 minutes time intervals, then for $T_c = 1, 5, 15$ minutes, the knowledge of the average rate in the next slot corresponds to the knowledge of the actual rate. Instead, for $T_c = 30$ minutes,

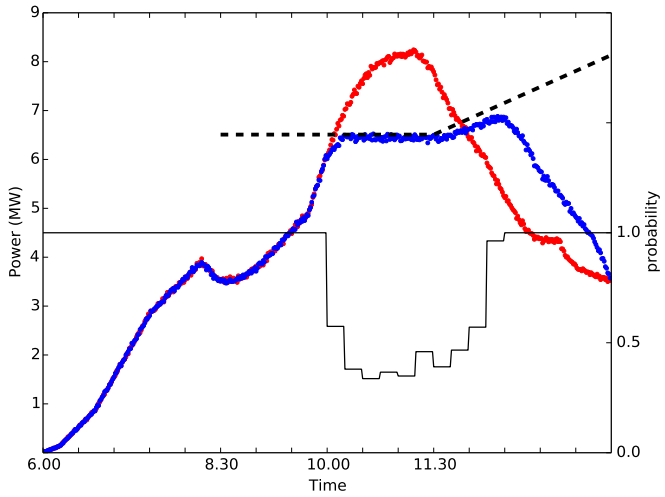

Figure 9: Instantaneous absorbed power (with and without the applied control), and the computed activation probability $p(t)$.

the average arrival rate is a bad predictor for the actual arrival rate.

The lower plots in figures 10 and 11 show the same metrics when the simple estimators described in Section 4 are used. In this case, utilization is expected to increase, due to the fact that the controller will usually underestimate λ_{k+1} for $t < 10.00$am (because the arrival rate keeps increasing), so it will select a too high probability p_{k+1} allowing the activation of a number of appliances larger than the correct value. This error has larger consequences for small q, when a higher percentage of appliances is activated through the probabilistic control. For T_c different from 30 minutes, there is only a slight increase in the utilization, but still it has a remarkable effect on the overload probability. In particular for $q < 0.1$ the bound is no more satisfied. For $T_c = 30$ minutes, the controller uses the average rate measured in $[9.30\text{am}, 10.00\text{am}]$ to estimate the arrival rate during the interval $[10.00\text{am}, 10.30\text{am}]$ with about a 20% of relative error. This justifies the bad performance achieved in this scenario. We observe that, even without using better estimators, one could simply counteract the estimation errors, for example by reducing p_{k+1} with a given factor corresponding to the maximum variability of the arrival rate from a control slot to the following one.

A final aspect to evaluate is how the communication overhead at the controller depends on the request arrival rate, the control interval $[T_{sc}, T_e]$ and the parameters q and T_c. Here we refer to the scenario when the controller is deployed at the DSO and broadcast functionalities are available at data concentrators (as discussed in Section 2). Let η be the number of data concentrators. Each query forwarded to the controller during the interval $[T_{sc}, T_e]$ generates an ACK message and during this interval the controller needs to send one message

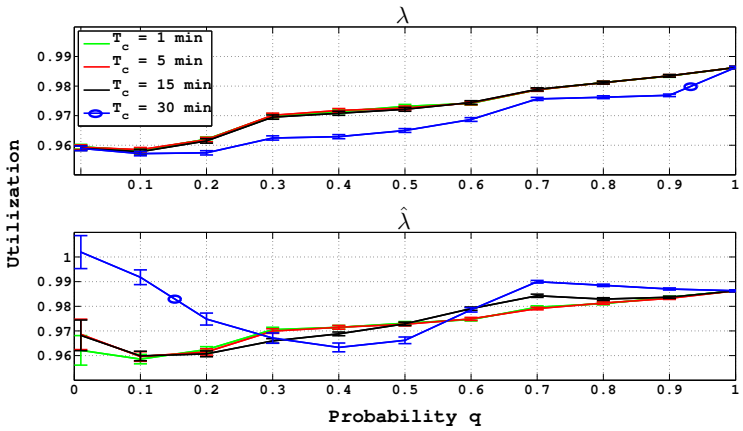

Figure 10: Resources utilization at 10.26am.

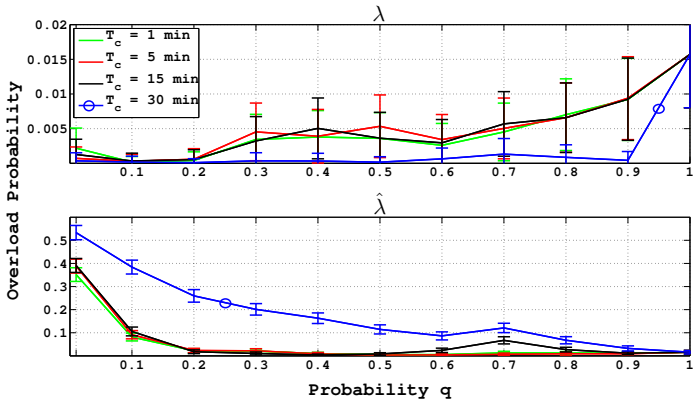

Figure 11: Probability to exceed $\bar{P}$ at 10.26am.

every T_c to each of the η concentrators. Then, the expected number of messages at the controller is:

$$2\int_{T_{sc}}^{T_e} q\lambda(t)\mathrm{d}t + \frac{T_e - T_{sc}}{T_c}\eta \tag{15}$$

An alternative solution is to rely only on queries. In this case the expected number of queries is $2\int_{T_{sc}}^{T_e}\lambda(t)\mathrm{d}t + \eta$, because all the queries will be forwarded to the controller and one message needs to be sent to all the concentrators (and then broadcast to all the appliances) to specify the interval of control. Fig. 12 plots the expected number of messages obtained from (15) for different values of the number of concentrators η and $T_c = 15$ minutes, as well as for the solution relying only on queries (the horizontal line). Different values of T_c would simply shift up or down the costs without changing the slope. The intersection between

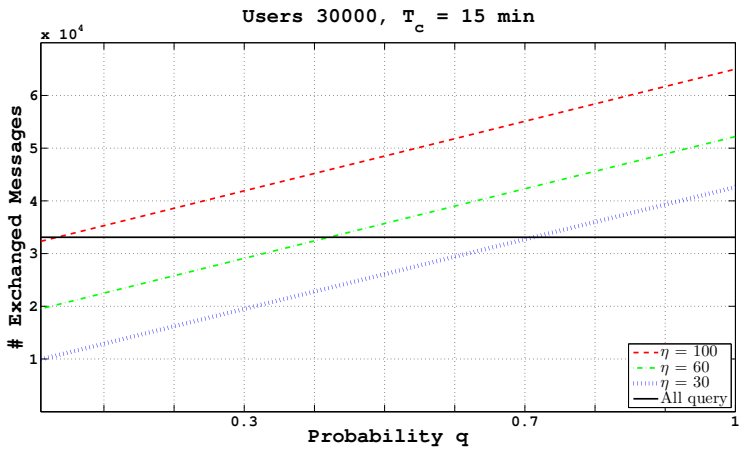

Figure 12: Expected number of exchanged messages for different numbers of data concentrators.

one of the oblique lines and the horizontal one determines the q value for which the two approaches have the same communication overhead. For smaller values of q our solution is more advantageous in this regard, and obviously in terms of privacy.

6. Conclusions

In this paper we propose a DLC scheme for smart grids designed using well-established teletraffic tools for direct load control, which can provide probabilistic guarantees on the power demand in the controlled zone. The scheme can work with a large number of dumb appliances, and can be configured for providing the desired trade-off between resource utilization, communication overhead and privacy.

The main idea is to control a class of electric appliances by combining a centralized query-response system with a probabilistic system able to take local decisions. The highest is the ratio between the activation requests that are locally processed and the ones that are forwarded to the controller, the lowest is the information leakage on user habits and the communication overheads, at the expense of control efficiency.

7. References

[1] L. Mathieu, S. Koch, D. Callaway, State estimation and control of electric loads to manage real-time energy imbalance, Power Systems, IEEE Trans. on 28 (1) (2013) 430–440.

[2] H. Hao, Y. Lin, A. Kowli, P. Barooah, S. Meyn, Ancillary service to the grid through control of fans in commercial building hvac systems, Smart Grid, IEEE Trans. on 5 (4) (2014) 2066–2074. doi:10.1109/TSG.2014.2322604.

[3] W. Kempton, S. E. Letendre, Electric vehicles as a new power source for electric utilities, Transportation Research Part D: Transport and Environment 2 (3) (1997) 157 – 175. doi:http://dx.doi.org/10.1016/S1361-9209(97)00001-1.

[4] Z. Ma, D. S. Callaway, I. A. Hiskens, Decentralized charging control of large populations of plug-in electric vehicles, IEEE Transactions on Control Systems Technology 21 (1) (2013) 67–78. doi:10.1109/TCST.2011.2174059.

[5] S. P. Meyn, P. Barooah, A. Busić, J. Ehren, Ancillary service to the grid from deferrable loads: The case for intelligent pool pumps in florida, in: IEEE CDC, 2013, pp. 6946–6953.

[6] Florida power and light, oncall savings program.
URL https://www.fpl.com/save/programs/on-call.html

[7] A. Benegiamo, P. Loiseau, G. Neglia, Dissecting Demand Response Mechanisms: the Role of Consumption Forecasts and Personalized Offers, in: Proc. of the 2016 Americal Control Conference (ACC 2016), 2016.

[8] R. Carli, M. Dotoli, R. Pellegrino, A hierarchical decision-making strategy for the energy management of smart cities, IEEE Transactions on Automation Science and Engineering PP (99) (2016) 1–19. doi:10.1109/TASE.2016.2593101.

[9] D. Croce, F. Giuliano, I. Tinnirello, A. Galatioto, M. Bonomolo, M. Beccali, G. Zizzo, Overgrid: A fully distributed demand response architecture based on overlay networks, IEEE Transactions on Automation Science and Engineering PP (99) (2016) 1–11. doi:10.1109/TASE.2016.2621890.

[10] T. Ganu, D. P. Seetharam, V. Arya, R. Kunnath, J. Hazra, S. A. Husain, L. C. De Silva, S. Kalyanaraman, nplug: A smart plug for alleviating peak loads, in: Proc. of the 3rd Intl Conference on Future Energy Systems: Where Energy, Computing and Communication Meet, e-Energy '12, ACM, New York, NY, USA, 2012, pp. 30:1–30:10.

[11] Y. Ghiassi-Farrokhfal, S. Keshav, C. Rosenberg, Toward a realistic performance analysis of storage systems in smart grids, Smart Grid, IEEE Trans. on PP (99) (2014) 1–1. doi:10.1109/TSG.2014.2330832.

[12] O. Ardakanian, S. Keshav, C. Rosenberg, On the use of teletraffic theory in power distribution systems, in: Future Energy Systems: Where Energy, Computing and Communication Meet (e-Energy), 2012 Third International Conference on, 2012, pp. 1–10.

[13] I. Tinnirello, G. Neglia, L. Giarre, G. D. Bella, J. M. Alain, M. Ippolito, Large scale control of deferrable domestic loads in smart grids, IEEE Transactions on Smart Grid PP (99) (2016) 1–1. doi:10.1109/TSG.2016.2563039.

[14] G. Neglia, G. D. Bella, L. Giarré, I. Tinnirello, Scalable and privacy-preserving admission control for smart grids, in: Prof. of the 54th IEEE Conference on Decision and Control (CDC), 2015, pp. 5233–5238. doi:10.1109/CDC.2015.7403038.

[15] N. Ruiz, I. Cobelo, O. J., A Direct Load Control Model for Virtual Power Plant Management, IEEE Trans. on Power Systems 24 (2) (2009) 959–966.

[16] An Overview to New PLC Applications and New Challenges - Maxium Integrated Products.
URL http://www.ieee-isplc.org/2011/Razazian_talk.pdf

[17] F. Kelly, E. Yudovina, Stochastic Networks, Cambridge University Press, 2014.

[18] C. Chang, Performance Guarantees in Communication Networks, Performance Guarantees in Communication Networks, Springer London, 2000.

[19] J. Widén, E. Wäckelgård, A high-resolution stochastic model of domestic activity patterns and electricity demand, Applied Energy 87 (6) (2010) 1880 – 1892. doi:http://dx.doi.org/10.1016/j.apenergy.2009.11.006.

[20] R. Miceli, Sustainable development and energy saving laboratory., Tech. rep., DIEET - University of Palermo (2007).

Appendix A. On the Frontiers

If we choose a control setting (p, n) and there are actually n appliances activated in the system through the query-response mechanism, then the expected power consumption is

$$\mathbb{E}[P] = (n + p(1-q)D\lambda)\mathbb{E}[X]\,. \tag{A.1}$$

We say that a control setting uses the resources more efficiently (shortly, it is more efficient) than another, if it can sustain a larger expected power demand without violating the bound. The linear approximation for evaluating the frontiers of the acceptance regions given in Eq. (10) leads to interesting consequences about efficiency, because it implies that all the pairs (p, n) on the frontiers have the same efficiency independently from q. This result is counter-intuitive: we could expect that the query-response control offers a better handle on the total power consumption, because the exact number of working appliances is known, and only the randomness of individual power absorption determines the variability of power consumption. On the other hand, the probabilistic control has another source of variability, i.e. the number of appliances actually admitted (that is a Poisson random variable). In this section we are going to show that this is the case, and the independency is simply and artefact of the linear approximation.

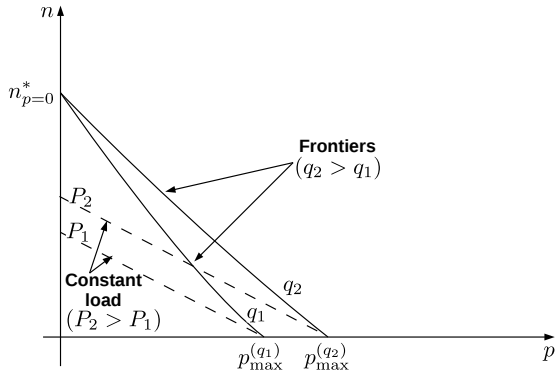

Figure A.13: Qualitative behavior of the frontiers. The segments are the geometric loci with constant expected power consumption.

The first observation is that the frontiers are not segments but in any case they are convex curves. Indeed, it can be shown from Eq. (8) that the acceptance region is concave because its complement is the intersection of a family of half-planes and then convex. Moreover, for $p = 0$ the maximum number of appliances that can be admitted does not depend on q, then all the frontiers intersect the y-axis in the same point $(0, n^*_{p=0})$. Fig. A.13 shows then a qualitative representation of what the frontiers look like. The loci with constant expected power consumption are characterized by

$$n + p(1-q)D\lambda = \text{const.}$$

We compare the slope of such segments $(-(1-q)D\lambda)$ with the slopes of the tangents to the frontiers. Given a pair (p, n) on a frontier, let $s^* \geq 0$ be a value at which the infimum of $nM_X(s) + p(1-q)\lambda D\left(e^{M_X(s)} - 1\right)$ is attained. The tangent to the frontier in (p, n) has slope:

$$-(1-q)\lambda D\frac{e^{M_X(s^*)} - 1}{M_X(s^*)} \leq -(1-q)\lambda D, \tag{A.2}$$

because for any x it holds $e^x \geq x + 1$. Taking into account these considerations, we have plotted in Fig. A.13 two loci with constant power demand (dashed lines). The figure confirms then our intuition: for a given frontier (a given q value), the larger n, the higher the efficiency. Despite all these considerations, as Fig. A.13 shows and Eq. (10) justifies analytically, this effect is negligible.

There is another aspect to be mentioned. We have assumed above that by selecting a pair (p, n) we can actually have n appliances activated through the query-response system, but this may not be the case if q is small. In particular if $q\lambda D << n$, the number of appliances activated through the query-response system will be smaller than n most of the time. Observe in fact that $q\lambda D$ is the expected number of requests to the controller during an interval n. If such number is much smaller than n, the cap will be ineffective most of the time.

Practically speaking the maximum value of n to be considered for a given q is $q\lambda D$. This remark is reflected in our way to set n, see Sec. 4.

We conclude this appendix with some additional consequences of Eq. (A.2) and the convex shape of the frontiers on the use of the linear approximation. If we consider a segment with slope $-(1-q)D\lambda$ passing by a point $(p_{\max}^{(q)}, 0)$, the segment is guaranteed to lie inside the acceptable region. On the contrary, a segment with the same slope passing by $(0, n^*_{p=0})$, would lie outside the acceptable region (even if very close to it). This is the reason why in Section 4 we have introduced $p_{\max}^{(q)}$ to configure the system instead to rely on Eq. (10).

Appendix B. Equivalence between the Energy-Bucket and the Queue

We show the equivalence for generic time-variant input/output rates. In particular we replace $\bar{P}$ with $T(t)$.

We write the equations for the two dynamics:

$$\frac{dL(t)}{dt} = \begin{cases} (T(t) - P(t))^+ & L(t) = 0 \\ T(t) - P(t) & 0 \le L(t) \le B \\ (P(t) - T(t))^+ & L(t) = B \end{cases} \tag{B.1}$$

$$\frac{dQ(t)}{dt} = \begin{cases} (P(t) - T(t))^+ & Q(t) = 0 \\ P(t) - T(t) & 0 \le Q(t) \le B \\ (T(t) - P(t))^+ & Q(t) = B \end{cases} \tag{B.2}$$

If $L(0) = L_0$ and $B(0) = B - L_0$, it can be easily checked that it will be $\frac{dQ(t)}{dt} = -\frac{dL(t)}{dt}$ for any $t \ge 0$. Then if $L(t)$ is the solution of (B.1) with $L(0) = L_0$, $Q(t) = B - L(t)$ is the solution of (B.2) with $Q(0) = B - L_0$. ■